



Published in final edited form as:

Autism Res. 2017 April ; 10(4): 631–647. doi:10.1002/aur.1714.

Auditory Processing in Noise Is Associated With Complex Patterns of Disrupted Functional Connectivity in Autism Spectrum Disorder

Fahimeh Mamashli, Sheraz Khan, Hari Bharadwaj, Konstantinos Michmizos, Santosh Ganesan, Keri-Lee A. Garel, Javeria Ali Hashmi, Martha R. Herbert, Matti Hämäläinen, and Tal Kenet

Department of Neurology, Massachusetts General Hospital, Boston, Massachusetts (F.M., S.K., H.B., K.M., S.G., K.-L.A.G., J.A.H., M.R.H., T.K.); Athinoula A. Martinos Center for Biomedical Imaging, MGH/MIT/Harvard, Boston, Massachusetts (F.M., S.K., H.B., K.M., S.G., K.-L.A.G., J.A.H., M.R.H., M.H., T.K.); Harvard Medical School, Boston, Massachusetts (F.M., S.K., H.B., K.M., S.G., K.-L.A.G., J.A.H., M.R.H., M.H., T.K.); McGovern Institute for Brain Research Massachusetts Institute of Technology, Boston, Massachusetts (S.K., K.M.); Department of Radiology, Massachusetts General Hospital, Boston, Massachusetts (M.H.); Department of Neuroscience and Biomedical Engineering, Aalto University School of Science Espoo, Finland (M.H.)

Abstract

Autism spectrum disorder (ASD) is associated with difficulty in processing speech in a noisy background, but the neural mechanisms that underlie this deficit have not been mapped. To address this question, we used magnetoencephalography to compare the cortical responses between ASD and typically developing (TD) individuals to a passive mismatch paradigm. We repeated the paradigm twice, once in a quiet background, and once in the presence of background noise. We focused on both the evoked mismatch field (MMF) response in temporal and frontal cortical locations, and functional connectivity with spectral specificity between those locations. In the quiet condition, we found common neural sources of the MMF response in both groups, in the right temporal gyrus and inferior frontal gyrus (IFG). In the noise condition, the MMF response in the right IFG was preserved in the TD group, but reduced relative to the quiet condition in ASD group. The MMF response in the right IFG also correlated with severity of ASD. Moreover, in noise, we found significantly reduced normalized coherence (deviant normalized by standard) in ASD relative to TD, in the beta band (14–25 Hz), between left temporal and left inferior frontal sub-regions. However, unnormalized coherence (coherence during deviant or standard) was significantly increased in ASD relative to TD, in multiple frequency bands. Our findings suggest increased recruitment of neural resources in ASD irrespective of the task difficulty, alongside a

Address for correspondence and reprints: Tal Kenet, Department of Neurology, Massachusetts General Hospital, Boston, MA. tal@nmr.mgh.harvard.edu.

Present address of Hari Bharadwaj is at Department of Speech, Language, and Hearing Sciences and Department of Biomedical Engineering, Purdue University, West Lafayette, Indiana, Konstantinos Michmizos is at Department of Computer Science, Rutgers University, Piscataway, New Jersey, and Javeria Ali Hashmi is at Department of Anesthesia Pain Management and Perioperative Medicine, Dalhousie University, Halifax, Nova Scotia, Canada.

Supporting Information

Additional Supporting Information may be found in the online version of this article at the publisher's website.

reduction in top-down modulations, usually mediated by the beta band, needed to mitigate the impact of noise on auditory processing.

Keywords

autism; MEG; auditory; noise; connectivity; feedback; top-down

Introduction

Autism spectrum disorder (ASD) is a pervasive neurodevelopmental disorder which is currently estimated to affect up to about 1:45 children in United States [Zablotsky et al., 2015]. ASD is characterized by a broad range of behavioral and perceptual features including reduced social interactions, language impairment and repetitive, or stereotyped behaviors [Rapin & Dunn, 2003; Siegal & Blades, 2003; Tager-Flusberg & Caronna, 2007]. Impaired language comprehension in ASD has been closely linked to abnormal auditory processing [Rapin & Dunn, 2003; Roberts, Flagg, & Gage, 2004; Roberts et al., 2008; Roberts et al., 2011; Siegal & Blades, 2003]. One of the prominent auditory features of ASD is increased awareness of environmental noises and difficulty in hearing speech in background noise [Boatman et al., 2001; Grandin & Scariano, 1986]. A theoretical model proposes that ASD is characterized as a “noisy” cortex due to high levels of endogenous neural noise; that is, increased ratio of excitation to inhibition [Rubenstein & Merzenich, 2003; Simmons et al., 2009]. Higher inter-trial variability has also been documented in ASD [Dinstein et al., 2012; Milne, 2011], suggesting that neural signatures in ASD are noisy and unreliable. However, how these hypotheses and observations might explain the impaired perception of noise in ASD has not been elucidated.

So far, research on auditory perception in noise in ASD has been quite sparse. A behavioral study that examined the influence of various noise maskers on speech perception in ASD found that individuals with high functioning autism (HFA) or Asperger’s syndrome (AS) have higher speech reception thresholds defined as speech-to-noise ratio than typically-developing (TD) young adults when the noise maskers contained temporal or spectro-temporal dips, but not in stationary noise [Alcantara, Weisblatt, Moore, & Bolton, 2004]. That behavioral study postulated that poor speech-in-noise perception of HFA/AS was due to either poor temporal resolution or top-down processing, and reduced ability to integrate information from glimpses present in the temporal dips in the noise. A reduced and delayed speech-evoked EEG response has been found in ASD compared to TD in both quiet and noise in another study [Russo, Zecker, Trommer, Chen, & Kraus, 2009], that suggested that the in-quiet responses in ASD resembled the in-noise responses in TD. This study also found a negative correlation between verbal abilities and evoked response latency in noise, and suggested that children with weak verbal abilities may have relatively poor cortical differentiation for speech, and impaired early auditory processing. Reduced ability to segregate concurrent sound streams might be another underlying reason for impaired speech in noise perception in ASD [Bhatara, Babikian, Laugeson, Tachdjian, & Sininger, 2013; Bouvet, Mottron, Valdois, & Donnadieu, 2016; DePape, Hall, Tillmann, & Trainor, 2012; Lepisto et al., 2009; Russo et al., 2009].

Together, these studies strongly support the hypothesis that auditory processing in noise is impaired in ASD, but the mechanisms mediating this impairment remain unmapped. In the current study, we examined the effects of background noise on early auditory processing in ASD using magnetoencephalography (MEG), to map the neurophysiological differences that may arise exclusively in the presence of background noise. To that end, we focused on the mismatch paradigm, which has been particularly useful in investigating auditory perception in autism [Gomot et al., 2006; Kasai et al., 2005; Lepisto et al., 2005; Roberts et al., 2010; Roberts et al., 2011]. When measured using EEG, the paradigm produces a negative peak, and this peak is referred to as the MMN (mismatch negativity). MEG measures a magnetic field, and the response is therefore labeled MMF (mismatch field) [Hari et al., 1984; Levanen, Ahonen, Hari, McEvoy, & Sams, 1996]. MMN/F is elicited pre-attentively by any discriminable change occurring in a sequence of repetitive standard stimuli [Näätänen & Alho, 1995]. The underlying neural generators of MMN/F for frequency deviations have been consistently found in bilateral temporal areas and the inferior frontal gyri (IFG) [Garrido, Kilner, Stephan, & Friston, 2009]. Intracranial studies in humans confirmed these neural generators [Halgren et al., 1995; Kropotov et al., 2000; Liasis, Towell, Alho, & Boyd, 2001; Rosburg et al., 2005]. MMN/F generation involves two functional processes: sensory memory mechanism related to temporal generators and an automatic attention-switching process related to the frontal generators [Giard, Perrin, Pernier, & Bouchet, 1990]. Importantly, it has been suggested that IFG contributes to a top-down process that modulates the deviance detection system in the temporal cortices [Doeller et al., 2003; Escera, Yago, Corral, Corbera, & Nunez, 2003; Hsiao, Cheng, Liao, & Lin, 2010; MacLean & Ward, 2014; Maess, Jacobsen, Schroger, & Friederici, 2007].

While the MMN/F has been studied extensively, using many variations, the mechanisms of deviance perception in noise are largely unknown, and less often studied. That said, it is known that noise does impact the MMN [Kozou et al., 2005; Muller-Gass, Marcoux, Logan, & Campbell, 2001; Shtyrov et al., 1998]. In parallel, speech perception in noise for TD populations has been found to be highly dependent on the contextual cues and top-down processing [Obleser & Kotz, 2010; Obleser, Wise, Dresner, & Scott, 2007]. Speech comprehension in noise is facilitated by increased activity in higher order cortical areas, and increased functional connectivity among them [Obleser et al., 2007] as well as enhanced frontal to temporal top-down feedback [Park, Ince, Schyns, Thut, & Gross, 2015]. Although the generation of the MMN/F may be less complex than speech processing, nevertheless similar mechanisms may be involved. It has been suggested that the frontal MMN/F generator may be involved in tuning the auditory change detection system by an involuntary contrast amplification mechanism [Opitz, 2002].

Here, we hypothesized that in the presence of noise, the IFG would play an important role in fine-tuning the temporal cortex to extract the signal from noise. We further hypothesized that in ASD, this top-down mechanism will be impaired. We based this hypothesis on substantial evidence that increased bottom-up and reduced top-down processing is characteristic of ASD [Cook, Barbalat, & Blakemore, 2012; Kenet et al., 2012; Khan et al., 2013; Kitzbichler et al., 2015; Mitchell, Mottron, Soulières, & Ropar, 2010; Takarae, Luna, Minschew, & Sweeney, 2014]. We further hypothesized that these top-down connectivity abnormalities will manifest in the beta band (13–30Hz) in particular. This hypothesis was derived from the

fact that beta band oscillations are most associated with feedback influences [Bastos, Vezoli, Bosman, et al., 2015; Bastos, Vezoli, & Fries, 2015; Wang, 2010]. To test our hypotheses, we collected MEG data from 19 ASD and 17 TD participants during an auditory frequency mismatch paradigm, once in quiet, and once with a noisy background, and measured the MMF response, as well as functional connectivity; both unnormalized and normalized, during both conditions.

Materials and Methods

Participants

Nineteen male subjects diagnosed with ASD with an average age of 13 (± 3) years and 17 matched TD male subjects with an average age of 12 (± 2) participated in this study. Subjects with ASD had a prior clinical diagnosis of ASD and met a cutoff of >15 on the Social Communication Questionnaire, Lifetime Version, and ASD criteria on the Autism Diagnostic Observation Schedule (ADOS) [Lord, Rutter, DiLavore, & Risi, 1999], administered by trained research personnel who had established inter-rater reliability. Individuals with autism related medical conditions (e.g., Fragile-X syndrome, tuberous sclerosis) and other known risk factors (e.g., premature birth) were excluded from the study. All typically developing participants were below threshold on the Social Communication Questionnaire and were confirmed to be free of any neurological or psychiatric conditions, and of substance use for the past 6 month, via parent and self-reports. The ASD and typically developing groups did not differ in verbal IQ, but differed slightly on non-verbal IQ ($P = 0.04$), measured with the Kaufman Brief Intelligence Test – II [Kaufman & Kaufman, 2004]. Handedness information was collected using Dean Questionnaire [Piro, 1998]. Only right-handed participants were included in the study. A summary of demographic information and behavioral scores are in Table 1. All research was in compliance with the MGH institutional review board, and all participants were consented in accordance with the approved protocol.

Experimental Paradigms

The standard mismatch stimulus was a complex tone consisted of ten sinusoidal tones starting at 500 Hz with 25% frequency increments between them. Tones were 50 ms long including 5 ms rise and 5 ms fall times. Participants were instructed to watch a self-selected silenced movie without subtitles on a 17-inch screen positioned 100 cm in front, and ignore the auditory stimulation. Tones were sequentially presented diotically using insert earphones (Etymotic, Elk Grove Village, IL) at a sound pressure level (SPL) of 70 dB with a stimulus onset-to-onset interval of 950 ms with 8% jitter. The deviant mismatch stimulus was a complex tone constructed by raising the frequency of each tone in the standard by 30%. Deviants occurred among standards with a relative frequency of 0.2 in a pseudorandomized fashion with the constraint that two deviants were separated by at least 3 standards and at most 7 standards. The experiment consisted of two blocks, one in quiet, and the other a repetition of the first block with ICRA noise, explained below [Dreschler, Verschuure, Ludvigsen, & Westermann, 2001]. Block presentation was randomized relative to one another and relative to blocks from other paradigms recorded in the same session. Each block consisted of 420 trials.

ICRA Noise

The ICRA noise consists of six-speaker babble noise, in the background. The exact characteristics of the noise are provided in Table 1 (track number 7) in [Dreschler et al., 2001]. The noise in this particular track only retains the long-term spectrum and broadband modulations of the speech. Thus, while it does have some speech characteristics, the different frequencies components of the noise have been modulated differently. Therefore, the noise is perceived as white noise with spectro-temporal dips, similarly to the one used previously in a behavioral study of processing speech in noise in ASD [Alcantara et al., 2004], which is the reason it was chosen as the background noise. We provide a 10 sec sample online through the following link (https://www.dropbox.com/s/8qckddvyhgymme4/ICRA_noise.wav?dl=0).

Structural MRI Data Acquisition and Processing

T1-weighted, high-resolution, magnetization-prepared rapid acquisition gradient-echo (MPRAGE) structural images were acquired on a 3.0 T Siemens Trio whole-body MRI scanner (Siemens Medical Systems, Erlangen, Germany) using a 32 channel head coil. The in-plane resolution was $1 \times 1 \text{ mm}^2$, slice thickness 1.3 mm with no gaps, and a repetition time/inversion time/echo time/flip angle 2530 ms/1100 ms/3.39 ms/7°. Cortical reconstruction and parcellations for each subject were generated using Freesurfer [Dale, Fischl, & Sereno, 1999; Fischl, Sereno, & Dale, 1999]. After correcting for topological defects, cortical surfaces were triangulated with dense meshes with ~130,000 vertices in each hemisphere. For visualization, the surfaces were inflated, thereby exposing the sulci [Dale et al., 1999].

MEG Data Acquisition

MEG data were acquired inside a magnetically shielded room (IMEDCO) using a whole-head VectorView MEG system (Elekta-Neuromag), comprised of 306 sensors arranged in 102 triplets of two orthogonal planar gradiometers and one magnetometer. The signals were filtered between 0.1 and 200 Hz and sampled at 600 Hz. The position and orientation of the head with respect to the MEG sensor array was recorded continuously with help of four head position indicator coils [Uutela, Taulu, & Hämäläinen, 2001]. To allow co-registration of the MEG and MRI data, the locations of three fiducial points (nasion and auricular points) that define a head-based coordinate system, a set of points from the head surface, and the sites of the four head position indicator coils were digitized using a Fastrak digitizer (Polhemus) integrated with the Vectorview system. The electrocardiography (ECG) and electrooculography (EOG) signals were recorded simultaneously to detect heartbeats as well as vertical and horizontal eye movement and blink artifacts, which were later used to identify cardiac and ocular events in signal space projection method. During data acquisition, online averages were computed from artefact-free trials to monitor data quality in real time. All off-line analysis was based on the saved raw data. In addition, 5 min of data from the room void of a subject were recorded before each experimental session for noise estimation purposes.

MEG Data Preprocessing and Motion Correction

MEG data were spatially filtered using the signal space separation method (Elekta-Neuromag Maxfilter software) to suppress noise generated by sources outside the brain [Taulu & Simola, 2006; Taulu, Kajola, & Simola, 2004]. Signal space separation also corrects for head motion between and within runs [Taulu et al., 2004]. Cardiac and ocular artefacts were removed by signal space projection [Gramfort et al., 2014]. The data were filtered between 0.1 and 140 Hz. The data were epoched into single trials lasting 1s, from 400 ms prior to stimulus onset to 600 ms after it. Epochs were rejected if the peak-to-peak amplitude during the epoch exceeded 1000 fT/cm and 3000 fT in any of the gradiometer and magnetometer channels, respectively. To maintain a constant signal-to-noise ratio across conditions and participants, the number of trials per condition per participant was fixed at 50 for standard and deviant, the minimum number of accepted trials that we had for each condition and participant. For participants that had more than 50 good trials, we selected 50 trials randomly from the available trials. The random indices for each subject were stored and same indices were used for both coherence and source localization analysis to reduce the variability effect across different epochs. For evoked-response analysis we filtered the data from 0.5 to 40 Hz.

Source Estimation

The geometry of each participant's cortical surface was reconstructed from the 3D structural MRI data using FreeSurfer software (<http://surfer.nmr.mgh.harvard.edu>). The cortical surface was decimated to a grid of 10,242 dipoles per hemisphere, corresponding to a spacing of approximately 5 mm between adjacent source locations on the cortical surface. The MEG forward solution was computed using a single-compartment boundary-element model (BEM) assuming the shape of the intracranial space [Hämäläinen & Sarvas, 1987]. The watershed algorithm was used to generate the inner skull surface triangulations from the T1-weighted MR images of each participant. Assuming head movements occurred only between runs and to compensate for these movements, the forward solutions for each run were computed and averaged [Uutela et al., 2001]. The cortical current distribution was estimated using minimum-norm estimate (MNE) software (<http://www.martinos.org/martinos/user-Info/data/sofMNE.php>) and assuming the orientation of the source to be fixed perpendicular to the cortical mesh. The noise-covariance matrix used to calculate the inverse operator was estimated from data collected without a subject present. To reduce the bias of the MNEs toward superficial currents, we used depth weighting, that is, adjusted the source covariance matrix to favor deep source locations [Lin, Belliveau, Dale, & Hämäläinen, 2006].

Inter-Subject Cortical Surface Registration for Group Analysis

Each participant's inflated cortical surface was registered to an average cortical representation (FsAverage in Free-Surfer) by optimally aligning individual sulcal-gyral patterns computed in freesurfer [Fischl, Sereno, & Dale, 1999]. We employed a surface based registration technique based on folding patterns because it provides more accurate inter-subject alignment of cortical regions than volume-based approaches [Fischl, Sereno, Tootell, et al., 1999; Van Essen & Dierker, 2007].

Regions of Interest (ROI) Identifications and Analysis

We selected the ROIs based on the previous findings on the neural generators of MMN/F [Garrido et al., 2009; Naatanen, Paavilainen, Rinne, & Alho, 2007; Rinne, Degerman, & Alho, 2005] and defined by a Freesurfer parcellation [Destrieux, Fischl, Dale, & Halgren, 2010], namely superior temporal gyrus (STG), middle temporal gyrus (MTG), and IFG including BA44, 45, and 47. In addition, we used an automatic routine to break each large label into smaller equal size sub-labels; that is, all sub-labels in temporal and frontal areas were of approximately the same size. In total we ended up 16 temporal and 9 frontal sub-labels. Our goal to break the labels into such small pieces was to increase the spatial specificity for further coherence analysis. Larger sub-labels can lead to signal cancellation due to the sulcus geometry, which in turns decreases the signal to noise ratio available for coherence analysis [Ahlfors et al., 2010].

Sub-Label Time Series Extraction

To compute coherence between the temporal sub-labels with frontal sub-labels each vertex inside every sub-label, were first averaged across vertices to generate the mean sub-label time course. To avoid signal cancellation, the averaging took into account the polarity mismatches that occur because of MNE estimate spreading across sources whose orientations were not aligned. This was done by flipping the polarity of the signals from sources that were oriented at greater than 90° relative to a principal direction of the cortical normals within the sub-label. This process results in 2D matrix, which are epochs by time.

Time Frequency Decomposition

The 2D epoched time series was then convolved with a dictionary of complex Morlet wavelets (each spanning seven cycles), resulting in three dimensional complex spectra epoch-time-frequency matrix ($S_k(t, f)$).

Functional Connectivity Computation

- A. Unnormalized coherence: The coherence between each temporal-frontal sub-label pair was computed for all frequencies between 8 Hz and 60 Hz for standard and deviant trials separately. Equal numbers of trials (50 per participant) were used. We use the term “unnormalized” for the coherence measure within a single condition (standard or deviant).
- B. Normalized coherence: To eliminate the statistical bias due to the non-Gaussian distribution of coherence values and unequal sample sizes, as well as the problem of spurious coherence [Sekihara, Owen, Trisno, & Nagarajan, 2011], we used normalized coherence, also referred to sometimes as Z-Coherence [Maris, Schoffelen, & Fries, 2007]. In this measure, the principal condition (Deviant, a total of 50 trials per participant) is normalized with respect to a baseline condition (Standard, a total of 160 trials per participant), which addresses the bias [e.g., Khan et al., 2013].

Statistical Analysis in Source Space, and MMF Calculation

- A. Standard versus deviant within group: We compared the responses to the standard and deviant tones at each sub-label (STG: nine sub-labels, MTG: seven sub-labels, IFG: nine sub-labels) and each group (TD and ASD) separately. The mean of absolute evoked responses from 100 to 300 ms was used for each participants and sub-label. Statistics in source space were done in three steps, and corrected for multiple comparisons. Step (1): Data from standard and deviant conditions were statistically compared using a paired *t*-test for sub-labels within each label (STG/MTG/IFG). Step (2): *P*-values were corrected for multiple comparisons using permutation statistics within each label (STG/MTG/IFG). To that end, we first permuted the two conditions (standard, deviant) and then counted the significant sub-labels within each label (STG/MTG/IFG). This process was repeated 20,000 times, resulting in a null distribution, as expected. This distribution was then statistically compared with the original number of significant sub-labels, which assigns the *P*-value to each label. Step (3): Lastly, *P*-values were additionally corrected at each hemisphere using Bonferroni method by a factor of 3, for the three labels. Figure S1 in SOM illustrates these steps.
- B. Quiet versus noise within group: Following our hypothesis considering the role of IFG in top-down control of temporal areas, we compared quiet to noise MMF results in the IFG (left, right), using a paired *t*-test. To extract the MMF, mean absolute values of standard responses were subtracted from deviant responses, averaged in time and also across all sub-labels. Time window of interest was selected from 175 to 225 ms according to the prior research demonstrating peak of MMF around 200 ms in children [Shafer, Morr, Kreuzer, & Kurtzberg, 2000].
- C. TD versus ASD: Similar as (B) except using a two-sample *t*-test as the test statistics.
- D. Lateralization within group: We selected the most statistically significant MMF response sub-label on right IFG and compared it to each sub-label on left using paired *t*-test. The selected time window of interest was similar as (B). *P*-values were corrected for multiple comparisons using permutation statistics.

Statistical Analysis of Functional Connectivity: Correction in Time, Frequency and Space

All statistics on the functional connectivity, measured using coherence, were carried out in three steps using the entire analyzed range: 50–300 ms in time, and all frequencies from 8 to 60 Hz. We first explain these steps between two assumed groups of comparisons: G1 and G2. Step (1): The time frequency map of each pair (temporal sub-labels with frontal sub-labels) was compared and corrected for multiple comparison using cluster-based statistics (a non-parametric method) [Maris & Oostenveld, 2007], (Fig. S2A–C). We used $P < 0.05$ as initial threshold, 1000 permutations and the test statistics used were either one-sample, two sample or a paired *t*-test depends on the particular comparison. The cluster statistics output is a *P*-value, cluster mass and cluster mask. The *P*-value shows whether the cluster is significant after multiple comparisons correction in time and frequency. The cluster mass is

the sum of the T -value of every vertex inside the cluster; a positive cluster mass means $G1 > G2$ and a negative means $G2 > G1$. The cluster mask is a matrix with values of either 0 or 1 covering the statistical plane (time by frequency); indicating whether that particular time and frequency are within the cluster (1) or not (0). Clusters at each pair was accepted (if $P < 0.05$) or not ($P > 0.05$). Two 2D matrix was generated: One for the condition of $G1 > G2$ and a second one for $G2 > G1$. Each element of the 2D matrix was set to zero if $P > 0.05$ for that particular temporal-frontal pair statistics. In the case of $P < 0.05$, we used cluster masses in the 2D matrix (Fig. S2C). At this stage we had a matrix with the size of 9×16 corresponding to 9 frontal and 16 temporal sub-labels for $G1 > G2$ and a similar matrix for $G2 > G1$ (Fig. S2D). The sum of the cluster masses of each significant pair of this 9×16 matrix was called “original total connectivity.” Step (2): To estimate null distribution of this original total connectivity, we permuted the $G1$ and $G2$ and conducted the cluster statistics ($G1$ vs. $G2$) at each temporal-frontal pair again. This step also correct for multiple comparisons in space (across all sub-labels) using maximum statistics (Fig. S2E). By permuting $G1$ and $G2$ data 1000 times and repeating the cluster statistics, we ended up a matrix of 1000 permutation \times 9 frontal \times 16 temporal values as null distribution for $G1 > G2$ and $G2 > G1$ (Fig. S2F). Step (3): The null distribution was compared with the non-permuted original total connectivity of 9 frontal \times 16 temporal matrix, resulting to a single P -value for $G1 > G2$ corrected in time, frequency and space. Using similar approach, a second P -value was assigned to $G2 > G1$ condition (Fig. S2G).

More specific details for each comparison are as follows:

- A.** Standard versus deviant within group: Normalized coherence (deviant normalized by standard) was used to assess the difference between standard and deviant for each condition (quiet and noise) and each hemisphere (left, right) and both groups (TD, ASD). One-sample t -test was used as the test statistics. Please note that the normalized coherence is a Z-score on the deviant versus standard comparison, which is normally distributed by definition. Therefore, we applied one-sample t -test on the normalized coherence.
- B.** Quiet versus noise within group: Normalized coherence (deviant normalized by standard) was compared between the quiet and noise conditions within the TD and ASD groups in both hemispheres. A paired t -test was used as the test statistics.
- C.** TD versus ASD during standard or deviant trials: Unnormalized coherence within standard or deviant was compared between TD and ASD group in quiet and noise and each hemisphere. Two sample t -test was used as the test statistics.
- D.** TD versus ASD, normalized coherence: We compared the normalized coherence (deviant normalized by standard) between the TD and ASD group, for each hemisphere, and each condition (quiet, noise). Two sample t -test was used as the test statistics.
- E.** Lateralization within group: Right temporal-frontal normalized coherences for each pair of sub-labels were subtracted from an anatomically comparable left hemisphere sub-labels pair, and one-sample t -test used as the test statistics.

MMF Correlation With ADOS Scores: Correction in Space

Step (1): Spearman correlation between the MMF of individual ASD subjects and the individual ADOS scores was estimated at the IFG sub-labels, selected based on our initial hypothesis (Fig. S3). Step (2): we corrected for multiple comparison across sub-labels (space) using permutations. Subjects were permuted and then got the absolute sum of r -values across all sub-labels. This process was repeated 10,000 times, giving the null distribution. This distribution was then statistically compared with the original unshuffled r -values, which assigns the P -value to the IFG label (Fig. S3).

Results

Mismatch Evoked Responses – Standard Versus Deviant Within Group

Over all conditions and groups, the MMF evoked responses localized to the right STG (rSTG), right IFG (rIFG), and right MTG (rMTG) (Fig. 1A). More specifically, in the quiet condition, there was a significant MMF in the rSTG and rIFG in both the TD ($P_{\text{rSTG}} = 0.006$, $P_{\text{rIFG}} = 0.05$) and the ASD ($P_{\text{rSTG}} = 0.006$, $P_{\text{rIFG}} = 0.02$) groups. In the rMTG, the TD group showed a significant MMF ($P_{\text{rMTG}} = 0.001$) while the ASD group showed a trend ($P_{\text{rMTG}} = 0.1$). Two major differences emerged in the noise condition relative to the quiet condition. First, the MMF in the rIFG disappeared in the ASD group ($P_{\text{rIFG}} = 0.4$), but not in the TD group ($P_{\text{rIFG}} = 0.03$). Second, the ASD group had significant mismatch effect in rMTG ($P_{\text{rMTG}} = 0.03$) and rSTG ($P_{\text{rSTG}} = 0.03$). In contrast, in the TD group, only the rSTG showed a significant MMF ($P_{\text{rSTG}} = 0.009$), while the rMTG showed a trend ($P_{\text{rMTG}} = 0.1$). Similar analyses in the left hemisphere did not yield any significant MMF responses in either group. The evoked responses to the deviant and standard tones for the TD and ASD groups in each condition (quiet, noise) separately are shown in Fig. S4 in SOM. The MMF response for both groups and conditions is shown in Fig. S5.

Mismatch Field Responses – Quiet Versus Noise Within Group

A direct comparison of MMF between quiet and noise condition in ASD group yielded a significant effect in rIFG ($P = 0.05$, $t(18) = 2$). Similar analysis in the TD group revealed no MMF difference between quiet and noise conditions.

Mismatch Field Responses – TD Versus ASD

Comparing the MMF between the TD and ASD groups revealed a significant group effect only in the noise condition, in the rIFG ($P = 0.05$, $t(34) = 2$), as shown in Fig. 1B. Similar analysis in the left IFG was not significant.

Mismatch Field Responses – Lateralization Within Group

In quiet, we found a right lateralization of the MMF for ASD group ($P = 0.03$), and a marginal significance for TD group ($P = 0.08$) in the IFG. In noise, only the TD group demonstrated a right lateralization effect in the IFG ($P = 0.03$).

Long-Range Normalized Functional Connectivity – Standard Versus Deviant Within Group

Within the TD group, we found increased left temporal-frontal normalized functional connectivity during deviant trials relative to standard trials, in both quiet ($P = 0.03$) and noise ($P = 0.01$) conditions. This difference emerged mostly in the beta and low gamma frequency bands (Fig. 2A,C). In contrast, within the ASD group, there was also increased left temporal-frontal normalized coherence during deviant trials relative to standard trials, again mostly in the beta band, but only in the quiet condition ($P = 0.004$, Fig. 2B). The effects were limited to the left hemisphere, and no significant difference was observed in the right hemisphere.

Long-Range Normalized Functional Connectivity – Quiet Versus Noise Within Group

We found a trend toward reduced normalized functional connectivity, in the noise condition relative to the quiet condition, between left temporal and frontal areas, in the ASD group ($P = 0.08$) (Fig. S6). Neither group showed an effect in the right hemisphere in the quiet versus noise condition comparison.

Long-Range Unnormalized Functional Connectivity – TD Versus ASD During Standard or Deviant Trials

In the quiet condition in the left hemisphere, evoked temporal-frontal unnormalized functional connectivity was stronger in the ASD group than in the TD group for both standard ($P = 0.03$) and deviant ($P = 0.05$) trials. This manifested exclusively and prominently in the gamma band (Fig. 3A,B). In the quiet condition in the right hemisphere, temporal-frontal unnormalized functional connectivity during standard (but not deviant) trials was increased in the ASD group relative to the TD group, mainly in alpha and beta bands ($P = 0.04$, Fig. 3C). In the noise condition, left temporal-frontal unnormalized functional connectivity was increased in the ASD group relative to the TD group, during both standard ($P = 0.07$) and deviant ($P = 0.05$) trials. In contrast to the quiet condition, this difference was mediated primarily by the beta band for standard trials, and by the gamma band for deviant trials (Fig. 3D,E).

Long-Range Normalized Functional Connectivity – TD Versus ASD

We did not find any significant differences between the TD and ASD groups in the quiet condition using normalized coherences. In contrast, in the noisy condition, we found significantly stronger normalized coherence in the TD group relative to the ASD group, in the left hemisphere only ($P = 0.05$, Fig. 4). The main effect driving the group difference was in the beta frequency band, in the 100–250 ms time window.

Long-Range Normalized Functional Connectivity –Lateralization Within Group

There was a strong left lateralization of temporal-frontal normalized functional connectivity in the ASD group in the quiet condition ($P = 0.004$, Fig. 5), and a trend in TD group ($P = 0.08$). In noise, no lateralization effect was found in either group.

Correlation Between Brain Responses and Behavioral Scores

The MMF response was significantly negatively correlated with the total ADOS scores only in the rIFG ($P=0.01$, Fig. 6). We did not find any correlation between ADOS scores and coherence values.

Discussion

The goal of the current study was to investigate the neuronal mechanisms underlying impaired auditory perception in the presence of noise in subjects with ASD. To that end, we investigated the cortical response to a passive auditory mismatch paradigm with and without background noise. We focused on the neural source generators of auditory change detection (MMF), and the spectro-temporal dynamics of the functional connectivity, measured using coherence, between the corresponding sources. In the quiet condition, there were no group differences in the MMF. For functional connectivity, unnormalized coherence was increased in the ASD group relative to the TD group across left temporal-frontal areas, in the gamma band, in response to both standard and deviant trials. In addition, right temporal-frontal unnormalized coherence was increased in response to standard trials in alpha and beta band in the ASD group relative to the TD group. In noise, abnormalities in the ASD group were documented in both the MMF and in functional connectivity measures. MMF responses (deviant vs. standard) in the ASD group were reduced relative to the TD group in the right IFG. Left temporal-frontal unnormalized coherences was increased in the ASD group relative to the TD group in beta band during standard trials, for the entire response time window, and in the gamma band during deviant trials in the later part of the time window. In addition, left temporal-frontal normalized coherences (deviant normalized by standard) were reduced in beta frequency band in the ASD group relative to the TD group during the noise condition. Lastly, we found a negative correlation between the ADOS scores that behaviorally assess the severity of ASD, and the MMF responses in right IFG.

In combination, our findings point at a dysfunction in the IFG in ASD, which is known to have a top-down role in general [Bar, 2003, 2009; Hwang, Velanova, & Luna, 2010; Iba & Sawaguchi, 2003; Johnston, Levin, Koval, & Everling, 2007] and in auditory processing in particular [Doeller et al., 2003; Opitz, 2002]. Prefrontal cortex is suggested to play a particular role in tuning the sensory system according to the processing demands [Roland, 1981, 1982]. In speech perception, it has been demonstrated that the degree to which IFG areas are engaged dictates how well listeners are able to extract speech in noisy listening environments [Bidelman & Howell, 2015]. Interestingly, in the auditory mismatch paradigm, previous fMRI studies on adults have demonstrated that the activity in inferior frontal area increases when the distinctiveness of the sound input decreases [Doeller et al., 2003; Opitz, 2002]. In a noisy environment, the distinctiveness of the deviant from the standard tone is reduced. Hence, MMF responses in IFG were expected to increase in the noisy condition relative to the quiet condition. In this study, we observed a preserved MMF response in the TD group rather than an increase. We believe this discrepancy may be due to age of participants (children vs. adults). When the MMF distinctiveness is reduced, our results suggest that in TD children, top-down connectivity remains constant, rather than increases. It is this effect that was missing in the ASD group in our study. In addition, the negative

correlation between MMF in rIFG and ADOS scores in the ASD group suggests those individuals who have greater trouble processing speech in noise also might be more impacted by autism.

We further hypothesize that reduced left frontal-temporal connectivity in the beta band in ASD suggests reduced feedback connectivity. It has been proposed that feedback and feedforward connections are mediated by distinct frequency bands. Specifically, the beta frequency band has been shown to primarily mediate feedback connections, while the gamma frequency band mediates primarily feedforward connections [Bastos, Vezoli, Bosman, et al., 2015; Bastos et al., 2015; Wang, 2010]. In the mismatch paradigm, beta band oscillations have been associated with novelty processing [Haenschel, Baldeweg, Croft, Whittington, & Gruzelier, 2000], via increased power to unexpected tones. In addition, recent EEG studies on healthy adults found increased phase-synchronization between temporal and prefrontal areas in beta band for the deviant tone than the standard tone [MacLean & Ward, 2014], which is interpreted as reflecting frontal top-down influences over temporal areas [Hsiao et al., 2010; MacLean & Ward, 2014]. Our interpretation of the current data is also consistent with our previous studies in ASD. Using graph theory, we previously found that network efficiency during resting state is increased in the gamma frequency band, but reduced in the beta frequency band [Kitzbichler et al., 2015]. Given the role of gamma band oscillations in mediating feedforward connectivity, this result was suggested to indicate an inherent increased feedforward and reduced feedback connectivity in ASD. The current findings align with this hypothesis, since the increased unnormalized coherence in both quiet and noise in the ASD group relative to the TD group was in fact restricted to the gamma band during deviant trials. Likewise, during a passive 25-Hz vibrotactile stimulation in the somatosensory cortex, using granger causality, we previously found increased feed-forward connectivity in ASD relative to TD, between primary and secondary somatosensory cortex and reduced mu-beta rhythm, which has been associated with feedback connectivity, [Khan et al., 2015]. In addition, our findings are in line with an extensive body of evidence, spanning both psychological and neurophysiological data suggesting reduced top-down processing in ASD [Bird, Catmur, Silani, Frith, & Frith, 2006; Cook et al., 2012; Frith, 2003; Khadem, Hossein-Zadeh, & Khorrami, 2015; Loth, Gomez, & Happe, 2010]. Taken together, we propose that in the presence of noise, temporal areas in subjects with ASD do not get regulated or fine-tuned properly by frontal feedbacks or top-down inputs, relative to the same stimulus without a noisy background. This interpretation may explain previous observation of reduced ability to segregate concurrent sound streams [Lepisto et al., 2009] as well as difficulty to perceive speech in the noisy environment [Alcantara et al., 2004]. This abnormality sits atop abnormally increased functional connectivity in ASD within a single condition, likely meaning that neural resources in ASD might be recruited more broadly even for simple tasks [Orekhova et al., 2014; Rinaldi, Perrodin, & Markram, 2008; Supekar et al., 2013].

Another finding of this study was that the direction of functional connectivity abnormalities in ASD depended on whether the coherence measures were unnormalized or normalized. When coherence measures were not normalized, every time there was a significant group difference, it was in the direction of increased coherence in the ASD group relative to the TD group. In contrast, when coherence measures were normalized, it was in the direction of

being lower for ASD than for TD. While results from unnormalized coherence measures, which are inherently biased [Maris et al., 2007] need to be interpreted cautiously, given the group difference, these results likely suggest that coherence abnormalities in ASD do not manifest in a simple manner. Without normalization, the increased coherence in ASD during the quiet and noise conditions might be interpreted as a more intense and more distributed cortical sensory response, which may reflect the general increase in sensory sensitivities in ASD and aforementioned increased recruitment of neural resources. In contrast, normalized coherence, which measures relative, rather than absolute, coherence differences, was reduced in ASD. This suggests that individuals with ASD do not differentiate between different conditions, and whereas TD individuals likely recruit more resources during more taxing stimuli, such as in the noise condition, this is not the case in ASD, and all conditions are perceived and processed as equally taxing. This result is also consistent with our prior study of local phase amplitude coupling in the fusiform face area in ASD, where we found it was unchanged across conditions in the ASD group (emotional faces vs. houses), but changed in the TD group [Khan et al., 2013]. It is also worth noting that in fMRI studies, coherence measures must always be normalized either by another condition, or by a baseline.

The results on lateralization of the differences, in both MMF and functional connectivity, are also worth noting. Although previous studies on the neural generators of MMF/N demonstrated activity in both left and right IFG [Doeller et al., 2003] and auditory processing abnormalities have been documented in both hemispheres in ASD [Kujala, Lepisto, & Naatanen, 2013], many studies documented a right lateralized MMF response in IFG [Giard et al., 1990; Naatanen et al., 2007; Opitz, 2002; Rinne et al., 2005]. In the current study, we found similar right lateralization of MMF in both groups in the quiet condition, and for the TD group in the noise condition. However, the lateralization results for the MMF were condition dependent, not group dependent. Thus, the origin of the lateralization here likely has to do with the properties of the MMF, as discussed above, rather than differences between the TD and ASD groups. In contrast, the lateralization results for the connectivity analysis were group dependent. We found a strong left lateralization of the temporal-frontal normalized coherence in the ASD group in both conditions, but only a trend in the TD group, and even the trend was only in the quiet condition, not the noise condition.

To reconcile these seemingly disparate lateralization findings for the evoked MMF versus coherence, it is important to first note that there are intrinsic differences between evoked response analysis and time-frequency analysis. While evoked responses provide averaged information in the low frequency domain (<10 Hz), the time-frequency analysis provides unaveraged information in both low and high frequency. Second, it is also important to note that coherence calculations are not sensitive to the amplitude of the signal, whereas the MMF is calculated exclusively using signal amplitude. Therefore, each of these methods is sensitive to different and complementary aspects of the cortical response. As such, these results most likely reflect complementary abnormalities in ASD. In the case of the MMF, the group difference was significant only in the noise condition, and there was no group difference in lateralization in the quiet, “baseline,” condition, where MMF was normal in the ASD group. This therefore likely taps into basic auditory processing abnormalities in ASD, which have been shown to be most pronounced in the right hemisphere previously [Edgar et

al., 2015; Haesen, Boets, & Wagemans, 2011; Oram Cardy, Flagg, Roberts, & Roberts, 2008; Roberts et al., 2010]. In contrast, the functional connectivity abnormalities measures using coherence were left lateralized in the ASD group regardless of condition, and were significant only in the ASD group. Left hemispheric abnormalities in ASD during a mismatch paradigm have been reported before. An fMRI study comparing the MMN between TD and ASD group found differences in the left hemisphere in IFG, anterior cingulate and mid orbitofrontal gyrus [Gomot et al., 2006]. Another MEG study demonstrated a negative correlation between MMF latency with the symptom severity in adults with ASD in the left hemisphere [Kasai et al., 2005]. In addition, auditory steady state responses in autism were exclusively diminished in left hemisphere and not right hemisphere [Wilson, Rojas, Reite, Teale, & Rogers, 2007]. In addition to these non-functional connectivity findings in ASD, prior fMRI and EEG studies found reduced left temporal-frontal functional connectivity in ASD during language comprehension task [Jochaut et al., 2015; Just, Cherkassky, Keller, & Minshew, 2004]. It is likely that the left hemispheric specific abnormalities in coherence in the ASD group are a manifestation of the role of left hemisphere in speech processing in general, which is well-known to be abnormal in ASD [Mody et al., 2013].

These findings might also be interpreted in light of the dual functional processes involved in the generation of the MMF [Giard et al., 1990]. It is possible that the evoked MMF abnormalities documented here in ASD arise due to a deficit with the sensory memory mechanism, which is more vulnerable in noise, while the coherence abnormalities documented here arise from a deficit in automatic attention switching, which is more generally impaired in ASD.

This study has several limitations. First, while the MMN/F has been long considered to be “pre-attentive,” there is now clear evidence that attention does influence the mismatch response [Auksztulewicz & Friston, 2015; Gomes et al., 2000]. In addition, attention modulates not only MMN/F amplitude, but also feedback connections from the upstream frontal and parietal areas to the auditory areas in MMN/F paradigm [Auksztulewicz & Friston, 2015]. Therefore, if attentional control in the ASD group was different from that of the TD group, a factor that is very difficult to monitor in a passive paradigm, this might be one of the contributors to the observed differences. That said, it is worth noting that by subjective observation, all participants seemed equally engaged in the watched silenced movie, regardless of group. Another limitation of the study relates to the lack of additional behavioral measures beyond the ADOS, and in particular auditory processing measures. Thus, it was not possible to directly correlate between neural signatures and behavioral measures of auditory processing in general, and auditory processing in noise in particular. Last, when interpreting results of unnormalized coherence measures in the gamma band in particular, it is important to keep in mind that artifacts from cranial muscles pose a serious problem for investigation of high-frequency brain activity in ongoing EEG and MEG of adults. This is because the magnitude of such activity may exceed magnitude of the cortical gamma by tens or even hundreds of times [Muthukumaraswamy, 2013]. It is possible that the muscular activity was stronger in ASD children due to potentially increased stress during MEG recordings. Another source of artifacts that suggests increased caution when interpreting coherence results in gamma oscillations comes from microsaccades [Carl, Acik,

Konig, Engel, & Hipp, 2012; Yuval-Greenberg, Tomer, Keren, Nelken, & Deouell, 2008]. That said, the primary and main results of this study were observed in the beta frequency band, which is less impacted by such artifacts, and the results for unnormalized coherence measures spanned frequencies outside of the gamma band. Thus, the interference of such artifacts with the final results is likely limited.

Conclusions

In summary, we investigated the neuronal mechanism of impaired auditory perception in the presence of noise in ASD. By examining the spatial and spectral characteristics of auditory change detection with and without noise, we found that in noise, ASD is characterized by a dysfunction in the inferior frontal gyrus in the cortex, which manifested in both the evoked response and in functional connectivity. Considering the role of the inferior frontal gyrus in fine tuning temporal cortex and beta band oscillations in feedback influences, our findings indicate that reduced feedback connections and consequent weak top-down processing likely contribute to auditory and language impairments in concomitant noise in ASD. Importantly, we found that the direction of abnormalities in coherence, reduced versus increased in ASD, depended on whether or not the measures were normalized by another condition. This indicates that it is essential to measure functional connectivity in ASD with and without normalization by a different condition, to truly map the neural abnormalities associated with the disorder. This result suggests that ASD individuals might recruit increased neural resources regardless of the difficulty associated with the task, and thus have a deficit in the relative recruitment of neural resources. Our results also support the noisy cortex hypothesis of ASD [Rubenstein & Merzenich, 2003]. Reduced feedback and increased recruitment of neural resources which is likely not well differentiated, would diminish the signal and allow increased noise from spontaneous fluctuations in brain activity that would be left unregulated. Such a scenario is consistent with recent findings on language deficits in ASD [Edgar et al., 2015], and findings of increased trial-to-trial variability in the cortical response in ASD, which is also a measure of signal-to-noise ratio in the brain. Taken together with previous findings, these results also support the hypothesis that weak top-down processing in response to more challenging inputs is not limited to a particular sensory system in ASD, but, rather, is a global feature of ASD cortical processing.

Acknowledgments

This work was supported by grants from the Nancy Lurie Marks Family Foundation (T.K., S.K.), Autism Speaks (T.K.), The Simons Foundation (SFARI 239395, T.K.), The National Institute of Child Health and Development (R01HD073254, T.K.), The National Centre for Research Resources (P41EB015896, M.S.H.), National Institute for Biomedical Imaging and Bioengineering (5R01EB009048, M.S.H.), and the Cognitive Rhythms Collaborative: A Discovery Network (NFS 1042134, M.S.H.). Article needs to be deposited in PMC. The authors declare no competing financial interests.

References

Ahlfors SP, Han J, Lin FH, Witzel T, Belliveau JW, Hamalainen MS, Halgren E. Cancellation of EEG and MEG signals generated by extended and distributed sources. *Human Brain Mapping*. 2010; 31:140–149. DOI: 10.1002/hbm.20851 [PubMed: 19639553]

- Alcantara JI, Weisblatt EJ, Moore BC, Bolton PF. Speech-in-noise perception in high-functioning individuals with autism or Asperger's syndrome. *Journal of Child Psychology and Psychiatry*. 2004; 45:1107–1114. DOI: 10.1111/j.1469-7610.2004.t01-1-00303.x [PubMed: 15257667]
- Auksztulewicz R, Friston K. Attentional enhancement of auditory mismatch responses: A DCM/MEG study. *Cerebral Cortex*. 2015; 25:4273–4283. DOI: 10.1093/cercor/bhu323 [PubMed: 25596591]
- Bar M. A cortical mechanism for triggering top-down facilitation in visual object recognition. *Journal of Cognitive Neuroscience*. 2003; 15:600–609. DOI: 10.1162/089892903321662976 [PubMed: 12803970]
- Bar M. The proactive brain: Memory for predictions. *Philosophical Transactions of the Royal Society of London Series B: Biological Sciences*. 2009; 364:1235–1243. DOI: 10.1098/rstb.2008.0310 [PubMed: 19528004]
- Bastos AM, Vezoli J, Bosman CA, Schoffelen JM, Oostenveld R, Dowdall JR, ... Fries P. Visual areas exert feedforward and feedback influences through distinct frequency channels. *Neuron*. 2015; 85:390–401. DOI: 10.1016/j.neuron.2014.12.018 [PubMed: 25556836]
- Bastos AM, Vezoli J, Fries P. Communication through coherence with inter-areal delays. *Current Opinion in Neurobiology*. 2015; 31:173–180. DOI: 10.1016/j.conb.2014.11.001 [PubMed: 25460074]
- Bhatara A, Babikian T, Laugeson E, Tachdjian R, Slinger YS. Impaired timing and frequency discrimination in high-functioning autism spectrum disorders. *Journal of Autism and Developmental Disorders*. 2013; 43:2312–2328. DOI: 10.1007/s10803-013-1778-y [PubMed: 23386117]
- Bidelman GM, Howell M. Functional changes in inter- and intra-hemispheric cortical processing underlying degraded speech perception. *Neuroimage*. 2015; 124:581–590. DOI: 10.1016/j.neuroimage.2015.09.020 [PubMed: 26386346]
- Bird G, Catmur C, Silani G, Frith C, Frith U. Attention does not modulate neural responses to social stimuli in autism spectrum disorders. *Neuroimage*. 2006; 31:1614–1624. DOI: 10.1016/j.neuroimage.2006.02.037 [PubMed: 16616862]
- Boatman D, Alidoost M, Gordon B, Lipsky F, Zimmerman W. Tests of auditory processing differentiate Asperger's syndrome from high-functioning autism. *Annals of Neurology*. 2001; 50:S95–S95.
- Bouvet L, Mottron L, Valdois S, Donnadieu S. Auditory stream segregation in autism spectrum disorder: Benefits and downsides of superior perceptual processes. *Journal of Autism and Developmental Disorders*. 2016; 46:1553–1561. DOI: 10.1007/s10803-013-2003-8 [PubMed: 24281422]
- Carl C, Acik A, Konig P, Engel AK, Hipp JF. The saccadic spike artifact in MEG. *NeuroImage*. 2012; 59:1657–1667. DOI: 10.1016/j.neuroimage.2011.09.020 [PubMed: 21963912]
- Cook J, Barbalat G, Blakemore SJ. Top-down modulation of the perception of other people in schizophrenia and autism. *Frontiers in Human Neuroscience*. 2012; 6:175. doi: 10.3389/fnhum.2012.00175 [PubMed: 22715325]
- Dale AM, Fischl B, Sereno MI. Cortical surface-based analysis. I. Segmentation and surface reconstruction. *Neuroimage*. 1999; 9:179–194. [PubMed: 9931268]
- DePape AM, Hall GB, Tillmann B, Trainor LJ. Auditory processing in high-functioning adolescents with autism spectrum disorder. *PLoS One*. 2012; 7:e44084. doi: 10.1371/journal.pone.0044084 [PubMed: 22984462]
- Destrieux C, Fischl B, Dale A, Halgren E. Automatic parcellation of human cortical gyri and sulci using standard anatomical nomenclature. *NeuroImage*. 2010; 53:1–15. DOI: 10.1016/j.neuroimage.2010.06.010 [PubMed: 20547229]
- Dinstein I, Heeger DJ, Lorenzi L, Minshew NJ, Malach R, Behrmann M. Unreliable evoked responses in autism. *Neuron*. 2012; 75:981–991. DOI: 10.1016/j.neuron.2012.07.026 [PubMed: 22998867]
- Doeller CF, Opitz B, Mecklinger A, Krick C, Reith W, Schroger E. Prefrontal cortex involvement in preattentive auditory deviance detection: Neuroimaging and electrophysiological evidence. *Neuroimage*. 2003; 20:1270–1282. DOI: 10.1016/S1053-8119(03)00389-6 [PubMed: 14568496]

- Dreschler WA, Verschuure H, Ludvigsen C, Westermann S. ICRA noises: Artificial noise signals with speech-like spectral and temporal properties for hearing instrument assessment. *International Collegium for Rehabilitative Audiology*. 2001; 40:148–157. [PubMed: 11465297]
- Edgar JC, Khan SY, Blaskey L, Chow VY, Rey M, Gaetz W, ... Roberts TP. Neuromagnetic oscillations predict evoked-response latency delays and core language deficits in autism spectrum disorders. *Journal of Autism and Developmental Disorders*. 2015; 45:395–405. DOI: 10.1007/s10803-013-1904-x [PubMed: 23963591]
- Escera C, Yago E, Corral MJ, Corbera S, Nunez MI. Attention capture by auditory significant stimuli: Semantic analysis follows attention switching. *European Journal of Neuroscience*. 2003; 18:2408–2412. [PubMed: 14622204]
- Fischl B, Sereno MI, Dale AM. Cortical surface-based analysis. II: Inflation, flattening, and a surface-based coordinate system. *Neuroimage*. 1999; 9:195–207. [PubMed: 9931269]
- Fischl B, Sereno MI, Tootell RB, Dale AM. High-resolution intersubject averaging and a coordinate system for the cortical surface. *Human Brain Mapping*. 1999; 8:272–284. [PubMed: 10619420]
- Frith C. What do imaging studies tell us about the neural basis of autism? *Novartis Foundation Symposia*. 2003; 251:149–166. discussion 166–176, 281–197.
- Garrido MI, Kilner JM, Stephan KE, Friston KJ. The mismatch negativity: A review of underlying mechanisms. *Clinical Neurophysiology*. 2009; 120:453–463. DOI: 10.1016/j.clinph.2008.11.029 [PubMed: 19181570]
- Giard MH, Perrin F, Pernier J, Bouchet P. Brain generators implicated in the processing of auditory stimulus deviance: A topographic event-related potential study. *Psychophysiology*. 1990; 27:627–640. [PubMed: 2100348]
- Gomes H, Molholm S, Ritter W, Kurtzberg D, Cowan N, Vaughan HG Jr. Mismatch negativity in children and adults, and effects of an attended task. *Psychophysiology*. 2000; 37:807–816. [PubMed: 11117461]
- Gomot M, Bernard FA, Davis MH, Belmonte MK, Ashwin C, Bullmore ET, Baron-Cohen S. Change detection in children with autism: An auditory event-related fMRI study. *Neuroimage*. 2006; 29:475–484. [PubMed: 16115783]
- Gramfort A, Luessi M, Larson E, Engemann DA, Strohmeier D, Brodbeck C, ... Hämäläinen MS. MNE software for processing MEG and EEG data. *Neuroimage*. 2014; 86:446–460. DOI: 10.1016/j.neuroimage.2013.10.027 [PubMed: 24161808]
- Grandin, T., Scariano, MM. *Emergence: Labeled autistic*. New York: Arena Press; 1986.
- Haenschel C, Baldeweg T, Croft RJ, Whittington M, Gruzelier J. Gamma and beta frequency oscillations in response to novel auditory stimuli: A comparison of human electroencephalogram (EEG) data with in vitro models. *Proceedings of the National Academy of Sciences of the United States of America*. 2000; 97:7645–7650. DOI: 10.1073/pnas.120162397 [PubMed: 10852953]
- Haesen B, Boets B, Wagemans J. A review of behavioural and electrophysiological studies on auditory processing and speech perception in autism spectrum disorders. *Research in Autism Spectrum Disorders*. 2011; 5:701–714.
- Halgren E, Baudena P, Clarke JM, Heit G, Marinkovic K, Devaux B, ... Biraben A. Intracerebral potentials to rare target and distractor auditory and visual stimuli. II. Medial, lateral and posterior temporal lobe. *Electroencephalography and Clinical Neurophysiology*. 1995; 94:229–250. [PubMed: 7537196]
- Hämäläinen MS, Sarvas J. Feasibility of the homogeneous head model in the interpretation of neuromagnetic fields. *Physics in Medicine and Biology*. 1987; 32:91–97. [PubMed: 3823145]
- Hari R, Hamalainen M, Ilmoniemi R, Kaukoranta E, Reinikainen K, Salminen J, ... Sams M. Responses of the primary auditory cortex to pitch changes in a sequence of tone pips: Neuromagnetic recordings in man. *Neuroscience Letters*. 1984; 50:127–132. [PubMed: 6493619]
- Hsiao FJ, Cheng CH, Liao KK, Lin YY. Cortico-cortical phase synchrony in auditory mismatch processing. *Biological Psychology*. 2010; 84:336–345. DOI: 10.1016/j.biopsycho.2010.03.019 [PubMed: 20380866]
- Hwang K, Velanova K, Luna B. Strengthening of top-down frontal cognitive control networks underlying the development of inhibitory control: A functional magnetic resonance imaging

- effective connectivity study. *Journal of Neuroscience*. 2010; 30:15535–15545. DOI: 10.1523/JNEURO-SCI.2825-10.2010 [PubMed: 21084608]
- Iba M, Sawaguchi T. Involvement of the dorsolateral prefrontal cortex of monkeys in visuospatial target selection. *Journal of Neurophysiology*. 2003; 89:587–599. DOI: 10.1152/jn.00148.2002 [PubMed: 12522204]
- Jochaut D, Lehongre K, Saitovitch A, Devauchelle AD, Olasagasti I, Chabane N, ... Giraud AL. Atypical coordination of cortical oscillations in response to speech in autism. *Frontiers in Human Neuroscience*. 2015; 9:171. doi: 10.3389/fnhum.2015.00171 [PubMed: 25870556]
- Johnston K, Levin HM, Koval MJ, Everling S. Top-down control-signal dynamics in anterior cingulate and prefrontal cortex neurons following task switching. *Neuron*. 2007; 53:453–462. DOI: 10.1016/j.neuron.2006.12.023 [PubMed: 17270740]
- Just MA, Cherkassky VL, Keller TA, Minshew NJ. Cortical activation and synchronization during sentence comprehension in high-functioning autism: Evidence of underconnectivity. *Brain*. 2004; 127:1811–1821. [PubMed: 15215213]
- Kasai K, Hashimoto O, Kawakubo Y, Yumoto M, Kamio S, Itoh K, ... Kato N. Delayed automatic detection of change in speech sounds in adults with autism: A magnetoencephalographic study. *Clinical Neurophysiology*. 2005; 116:1655–1664. [PubMed: 15899591]
- Kaufman, AS., Kaufman, NL. Kaufman brief intelligence test. 2. Circle Pines, MN: AGS Publishing; 2004.
- Kenet T, Orekhova EV, Bharadwaj H, Shetty NR, Israeli E, Lee AK, ... Manoach DS. Disconnectivity of the cortical ocular motor control network in autism spectrum disorders. *Neuroimage*. 2012; 61:1226–1234. [PubMed: 22433660]
- Khadem A, Hossein-Zadeh GA, Khorrami A. Long-range reduced predictive information transfers of autistic youths in EEG sensor-space during face processing. *Brain Topography*. 2015; doi: 10.1007/s10548-015-0452-4
- Khan S, Gramfort A, Shetty NR, Kitzbichler MG, Ganesan S, Moran JM, ... Kenet T. Local and long-range functional connectivity is reduced in concert in autism spectrum disorders. *Proceedings of the National Academy of Sciences of the United States of America*. 2013; 110:3107–3112. [PubMed: 23319621]
- Khan S, Michmizos K, Tommerdahl M, Ganesan S, Kitzbichler MG, Zetino M, ... Kenet T. Somatosensory cortex functional connectivity abnormalities in autism show opposite trends, depending on direction and spatial scale. *Brain*. 2015; 138:1394–1409. [PubMed: 25765326]
- Kitzbichler MG, Khan S, Ganesan S, Vangel MG, Herbert MR, Hämäläinen MS, Kenet T. Altered development and multifaceted band-specific abnormalities of resting state networks in autism. *Biological Psychiatry*. 2015; 77:794–804. [PubMed: 25064418]
- Kozou H, Kujala T, Shtyrov Y, Toppila E, Starck J, Alku P, Näätänen R. The effect of different noise types on the speech and non-speech elicited mismatch negativity. *Hearing Research*. 2005; 199:31–39. DOI: 10.1016/j.heares.2004.07.010 [PubMed: 15574298]
- Kropotov JD, Alho K, Naatanen R, Ponomarev VA, Kropotova OV, Anichkov AD, Nechaev VB. Human auditory-cortex mechanisms of preattentive sound discrimination. *Neuroscience Letters*. 2000; 280:87–90. [PubMed: 10686384]
- Kujala T, Lepisto T, Naatanen R. The neural basis of aberrant speech and audition in autism spectrum disorders. *Neuroscience and Biobehavioral Reviews*. 2013; 37:697–704. DOI: 10.1016/j.neubiorev.2013.01.006 [PubMed: 23313648]
- Lepisto T, Kuitunen A, Sussman E, Saalasti S, Jansson-Verkasalo E, Nieminen-von Wendt T, Kujala T. Auditory stream segregation in children with Asperger syndrome. *Biological Psychology*. 2009; 82:301–307. DOI: 10.1016/j.biopsycho.2009.09.004 [PubMed: 19751798]
- Lepisto T, Kujala T, Vanhala R, Alku P, Huotilainen M, Naatanen R. The discrimination of and orienting to speech and non-speech sounds in children with autism. *Brain Research*. 2005; 1066:147–157. [PubMed: 16325159]
- Levanen S, Ahonen A, Hari R, McEvoy L, Sams M. Deviant auditory stimuli activate human left and right auditory cortex differently. *Cerebral Cortex*. 1996; 6:288–296. [PubMed: 8670657]

- Liasis A, Towell A, Alho K, Boyd S. Intracranial identification of an electric frontal-cortex response to auditory stimulus change: A case study. *Cognitive Brain Research*. 2001; 11:227–233. [PubMed: 11275484]
- Lin FH, Belliveau JW, Dale AM, Hämäläinen MS. Distributed current estimates using cortical orientation constraints. *Human Brain Mapping*. 2006; 27:1–13. DOI: 10.1002/hbm.20155 [PubMed: 16082624]
- Lord, C., Rutter, M., DiLavore, PC., Risi, S. *Autism diagnostic observation schedule—WPS (ADOS-WPS)*. Los Angeles, CA: Western Psychological Services; 1999.
- Loth E, Gomez JC, Happe F. When seeing depends on knowing: Adults with Autism Spectrum Conditions show diminished top-down processes in the visual perception of degraded faces but not degraded objects. *Neuropsychologia*. 2010; 48:1227–1236. DOI: 10.1016/j.neuropsychologia.2009.12.023 [PubMed: 20026140]
- MacLean SE, Ward LM. Temporo-frontal phase synchronization supports hierarchical network for mismatch negativity. *Clinical Neurophysiology*. 2014; 125:1604–1617. DOI: 10.1016/j.clinph.2013.12.109 [PubMed: 24508191]
- Maess B, Jacobsen T, Schroger E, Friederici AD. Localizing pre-attentive auditory memory-based comparison: Magnetic mismatch negativity to pitch change. *Neuroimage*. 2007; 37:561–571. DOI: 10.1016/j.neuroimage.2007.05.040 [PubMed: 17596966]
- Maris E, Oostenveld R. Nonparametric statistical testing of EEG- and MEG-data. *Journal of Neuroscience Methods*. 2007; 164:177–190. DOI: 10.1016/j.jneumeth.2007.03.024 [PubMed: 17517438]
- Maris E, Schoffelen JM, Fries P. Nonparametric statistical testing of coherence differences. *Journal of Neuroscience Methods*. 2007; 163:161–175. DOI: 10.1016/j.jneumeth.2007.02.011 [PubMed: 17395267]
- Milne E. Increased intra-participant variability in children with autistic spectrum disorders: Evidence from single-trial analysis of evoked EEG. *Frontiers in Psychology*. 2011; 2:51. doi: 10.3389/fpsyg.2011.00051 [PubMed: 21716921]
- Mitchell P, Mottron L, Soulieres I, Ropar D. Susceptibility to the Shepard illusion in participants with autism: Reduced top-down influences within perception? *Autism Research*. 2010; 3:113–119. DOI: 10.1002/aur.130 [PubMed: 20575110]
- Mody M, Manoach DS, Guenther FH, Kenet T, Bruno KA, McDougle CJ, Stigler KA. Speech and language in autism spectrum disorder: A view through the lens of behavior and brain imaging. *Neuropsychiatry*. 2013; 3:223–232.
- Muller-Gass A, Marcoux A, Logan J, Campbell KB. The intensity of masking noise affects the mismatch negativity to speech sounds in human subjects. *Neuroscience Letters*. 2001; 299:197–200. [PubMed: 11165769]
- Muthukumaraswamy SD. High-frequency brain activity and muscle artifacts in MEG/EEG: A review and recommendations. *Frontiers in Human Neuroscience*. 2013; 7:138. doi: 10.3389/fnhum.2013.00138 [PubMed: 23596409]
- Naatanen R, Alho K. Mismatch negativity – A unique measure of sensory processing in audition. *International Journal of Neuroscience*. 1995; 80:317–337. [PubMed: 7775056]
- Naatanen R, Paavilainen P, Rinne T, Alho K. The mismatch negativity (MMN) in basic research of central auditory processing: A review. *Clinical Neurophysiology*. 2007; 118:2544–2590. DOI: 10.1016/j.clinph.2007.04.026 [PubMed: 17931964]
- Obleser J, Kotz SA. Expectancy constraints in degraded speech modulate the language comprehension network. *Cerebral Cortex*. 2010; 20:633–640. DOI: 10.1093/cercor/bhp128 [PubMed: 19561061]
- Obleser J, Wise RJ, Dresner MA, Scott SK. Functional integration across brain regions improves speech perception under adverse listening conditions. *Journal of Neuroscience*. 2007; 27:2283–2289. DOI: 10.1523/JNEURO-SCI.4663-06.2007 [PubMed: 17329425]
- Opitz B. Differential contribution of frontal and temporal cortices to auditory change detection: fMRI and ERP results. *Neuroimage*. 2002; 15:167–174. DOI: 10.1006/nimg.2001.0970 [PubMed: 11771985]

- Oram Cardy JE, Flagg EJ, Roberts W, Roberts TP. Auditory evoked fields predict language ability and impairment in children. *International Journal of Psychophysiology*. 2008; 68:170–175. DOI: 10.1016/j.ijpsycho.2007.10.015 [PubMed: 18304666]
- Orehkova EV, Elsabbagh M, Jones EJ, Dawson G, Charman T, Johnson MH. EEG hyper-connectivity in high-risk infants is associated with later autism. *Journal of Neurodevelopmental Disorders*. 2014; 6:1. [PubMed: 24433325]
- Park H, Ince RA, Schyns PG, Thut G, Gross J. Frontal top-down signals increase coupling of auditory low-frequency oscillations to continuous speech in human listeners. *Current Biology*. 2015; 25:1649–1653. DOI: 10.1016/j.cub.2015.04.049 [PubMed: 26028433]
- Piro JM. Handedness and intelligence: Patterns of hand preference in gifted and nongifted children. *Developmental Neuropsychology*. 1998; 14:619–630.
- Rapin I, Dunn M. Update on the language disorders of individuals on the autistic spectrum. *Brain and Development*. 2003; 25:166–172. [PubMed: 12689694]
- Rinaldi T, Perrodin C, Markram H. Hyper-connectivity and hyper-plasticity in the medial prefrontal cortex in the valproic acid animal model of autism. *Frontiers in Neural Circuits*. 2008; 2:4. [PubMed: 18989389]
- Rinne T, Degerman A, Alho K. Superior temporal and inferior frontal cortices are activated by infrequent sound duration decrements: An fMRI study. *Neuroimage*. 2005; 26:66–72. DOI: 10.1016/j.neuroimage.2005.01.017 [PubMed: 15862206]
- Roberts TP, Cannon KM, Tavabi K, Blaskey L, Khan SY, Monroe JF, ... Edgar JC. Auditory magnetic mismatch field latency: A biomarker for language impairment in autism. *Biological Psychiatry*. 2011; 70:263–269. DOI: 10.1016/j.biopsych.2011.01.015 [PubMed: 21392733]
- Roberts TP, Flagg EJ, Gage NM. Vowel categorization induces departure of M100 latency from acoustic prediction. *Neuroreport*. 2004; 15:1679–1682. [PubMed: 15232306]
- Roberts TP, Khan SY, Rey M, Monroe JF, Cannon K, Blaskey L, ... Edgar JC. MEG detection of delayed auditory evoked responses in autism spectrum disorders: Towards an imaging biomarker for autism. *Autism Research*. 2010; 3:8–18. DOI: 10.1002/aur.111 [PubMed: 20063319]
- Roberts TP, Schmidt GL, Egeth M, Blaskey L, Rey MM, Edgar JC, Levy SE. Electrophysiological signatures: Magnetoencephalographic studies of the neural correlates of language impairment in autism spectrum disorders. *International Journal of Psychophysiology*. 2008; 68:149–160. DOI: 10.1016/j.ijpsycho.2008.01.012 [PubMed: 18336941]
- Roland PE. Somatotopical tuning of postcentral gyrus during focal attention in man. A regional cerebral blood flow study. *Journal of Neurophysiology*. 1981; 46:744–754. [PubMed: 7288462]
- Roland PE. Cortical regulation of selective attention in man. A regional cerebral blood flow study. *Journal of Neurophysiology*. 1982; 48:1059–1078. [PubMed: 7175557]
- Rosburg T, Trautner P, Dietl T, Korzyukov OA, Boutros NN, Schaller C, ... Kurthen M. Subdural recordings of the mismatch negativity (MMN) in patients with focal epilepsy. *Brain*. 2005; 128:819–828. DOI: 10.1093/brain/awh442 [PubMed: 15728656]
- Rubenstein JL, Merzenich MM. Model of autism: Increased ratio of excitation/inhibition in key neural systems. *Genes, Brain and Behavior*. 2003; 2:255–267.
- Russo N, Zecker S, Trommer B, Chen J, Kraus N. Effects of background noise on cortical encoding of speech in autism spectrum disorders. *Journal of Autism and Developmental Disorders*. 2009; 39:1185–1196. DOI: 10.1007/s10803-009-0737-0 [PubMed: 19353261]
- Sekihara K, Owen JP, Trisno S, Nagarajan SS. Removal of spurious coherence in MEG source-space coherence analysis. *IEEE Transactions on Bio-Medical Engineering*. 2011; 58:3121–3129. DOI: 10.1109/TBME.2011.2162514 [PubMed: 21824842]
- Shafer VL, Morr ML, Kreuzer JA, Kurtzberg D. Maturation of mismatch negativity in school-age children. *Ear and Hearing*. 2000; 21:242–251. [PubMed: 10890733]
- Shtyrov Y, Kujala T, Ahveninen J, Tervaniemi M, Alku P, Ilmoniemi RJ, Näätänen R. Background acoustic noise and the hemispheric lateralization of speech processing in the human brain: Magnetic mismatch negativity study. *Neuroscience Letters*. 1998; 251:141–144. [PubMed: 9718994]
- Siegal M, Blades M. Language and auditory processing in autism. *Trends in Cognitive Sciences*. 2003; 7:378–380. [PubMed: 12963465]

- Simmons DR, Robertson AE, McKay LS, Toal E, McAleer P, Pollick FE. Vision in autism spectrum disorders. *Vision Research*. 2009; 49:2705–2739. DOI: 10.1016/j.visres.2009.08.005 [PubMed: 19682485]
- Supekar K, Uddin LQ, Khouzam A, Phillips J, Gaillard WD, Kenworthy LE, ... Menon V. Brain hyperconnectivity in children with autism and its links to social deficits. *Cell Reports*. 2013; 5:738–747. DOI: 10.1016/j.celrep.2013.10.001 [PubMed: 24210821]
- Tager-Flusberg H, Caronna E. Language disorders: Autism and other pervasive developmental disorders. *Pediatric Clinics of North America*. 2007; 54:469–481. vi. DOI: 10.1016/j.pcl.2007.02.011 [PubMed: 17543905]
- Takarae Y, Luna B, Minshew NJ, Sweeney JA. Visual motion processing and visual sensorimotor control in autism. *Journal of the International Neuropsychological Society*. 2014; 20:113–122. DOI: 10.1017/S1355617713001203 [PubMed: 24365486]
- Taulu S, Kajola M, Simola J. Suppression of interference and artifacts by the signal space separation method. *Brain Topography*. 2004; 16:269–275. [PubMed: 15379226]
- Taulu S, Simola J. Spatiotemporal signal space separation method for rejecting nearby interference in MEG measurements. *Physics in Medicine and Biology*. 2006; 51:1759–1768. DOI: 10.1088/0031-9155/51/7/008 [PubMed: 16552102]
- Uutela K, Taulu S, Hämäläinen M. Detecting and correcting for head movements in neuromagnetic measurements. *Neuroimage*. 2001; 14:1424–1431. [PubMed: 11707098]
- Van Essen DC, Dierker DL. Surface-based and probabilistic atlases of primate cerebral cortex. *Neuron*. 2007; 56:209–225. DOI: 10.1016/j.neuron.2007.10.015 [PubMed: 17964241]
- Wang XJ. Neurophysiological and computational principles of cortical rhythms in cognition. *Physiological Reviews*. 2010; 90:1195–1268. DOI: 10.1152/physrev.00035.2008 [PubMed: 20664082]
- Wilson T, Rojas D, Reite M, Teale P, Rogers S. Children and adolescents with autism exhibit reduced MEG steady-state gamma responses. *Biological Psychiatry*. 2007; 62:192–197. DOI: 10.1016/j.biopsych.2006.07.002 [PubMed: 16950225]
- Yuval-Greenberg S, Tomer O, Keren AS, Nelken I, Deouell LY. Transient induced gamma-band response in EEG as a manifestation of miniature saccades. *Neuron*. 2008; 58:429–441. [PubMed: 18466752]
- Zablotsky B, Black L, Maenner M, Schieve L, Blumberg S. Estimated prevalence of autism and other developmental disabilities following questionnaire changes in the 2014 national health interview survey. *National Health Statistics Reports*. 2015; 87:1–21.

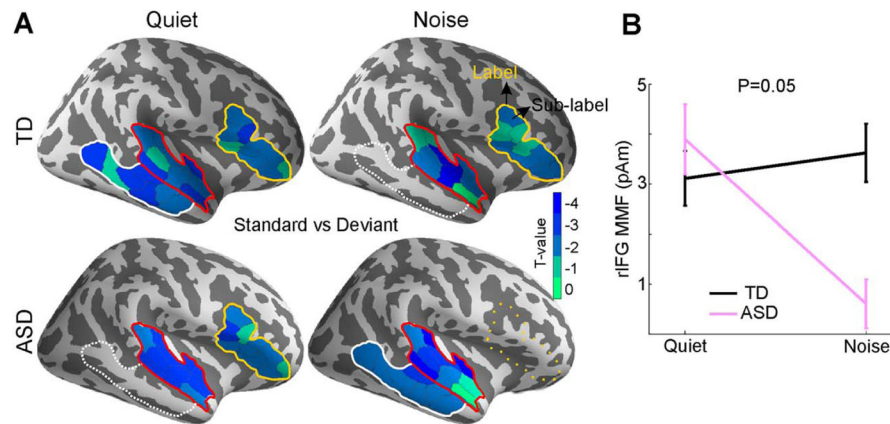


Figure 1.

(A) MMF response, obtained by contrasting the responses to deviant versus standard tones, in each condition (quiet and noise), and within each group. MMF was observed in the rSTG (red outline), rMTG (white outline), and rIFG (yellow outline). Solid outlines: $P < 0.05$ corrected. Dashed outlines: $P < 0.1$ (trend). Dotted outlines: No significant MMF. T-values of the sub-labels within each significant label are color-coded as indicated in the colorbar. (B) Mean and standard error of the MMF in rIFG for the TD and ASD group in the two conditions (quiet, noise).

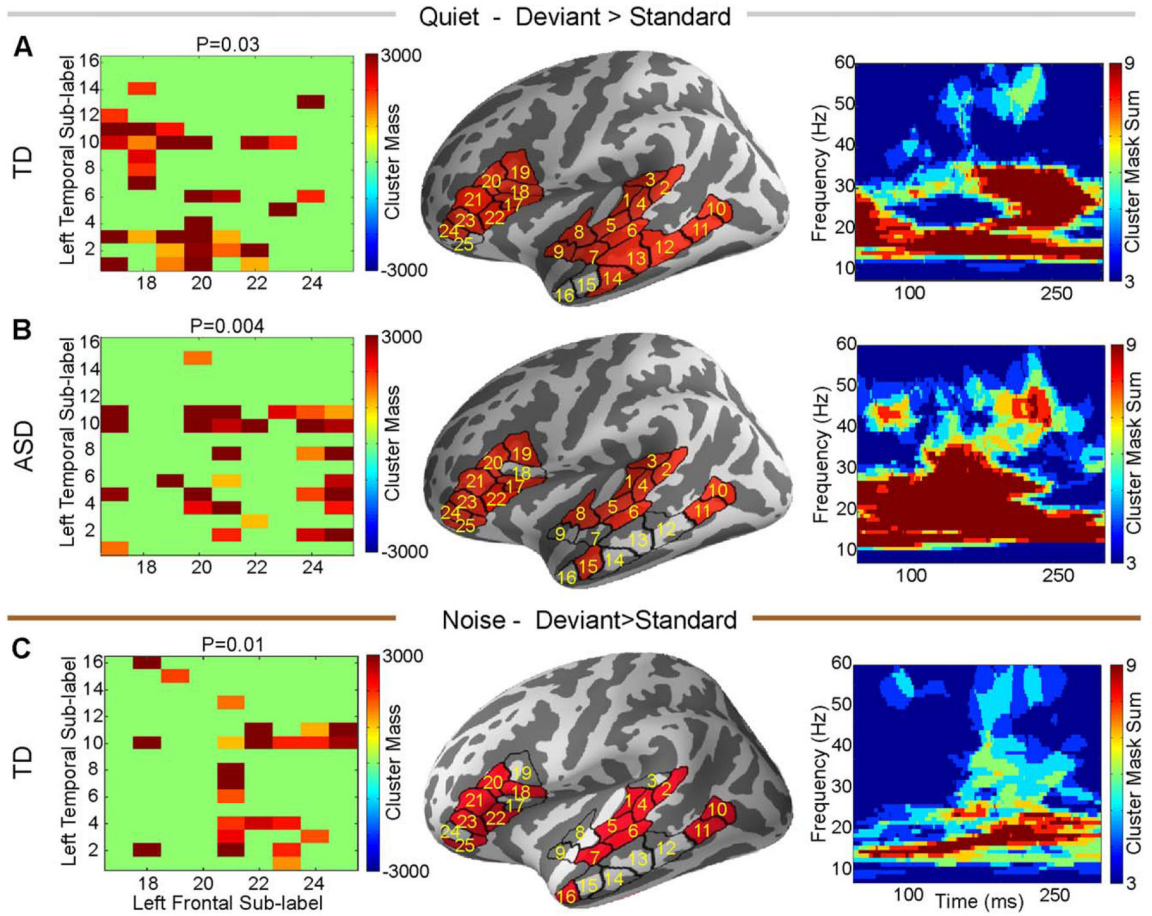


Figure 2. Deviant trials normalized by standard trials left temporal-frontal functional connectivity in quiet (A–B) and noise (C). Groups are marked on the individual panels. For each panel, the left column is the matrix of sub-label pairs that reached significance, the middle column shows those labels on the cortex, and the right column is the time frequency map of the sum of the cluster masks between the significant sub-labels from left column.

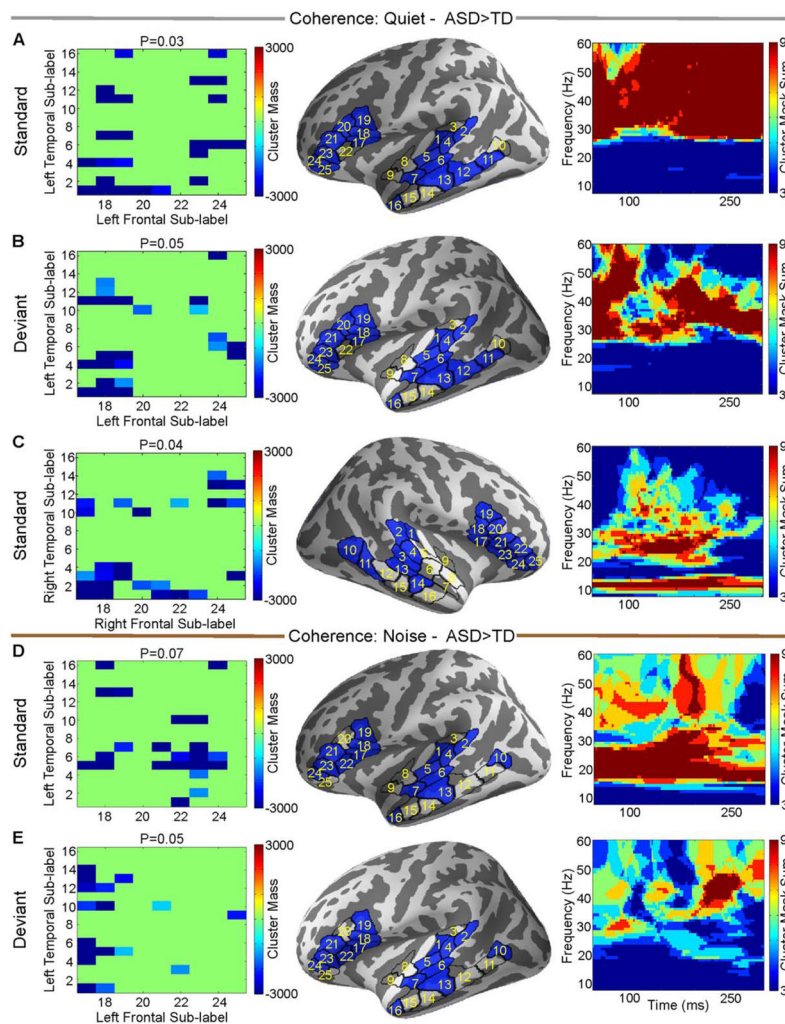


Figure 3.

TD versus ASD based on individual unnormalized coherence estimates within standard or deviant trials for the quiet condition (A–C) and the noise condition (D–E). Directions are marked on figure titles. For each panel, the left column is the matrix of sub-label pairs that reached significance, the middle column shows those labels on the cortex, and the right column is the time frequency map of the sum of the cluster masks between the significant sub-labels from left column.

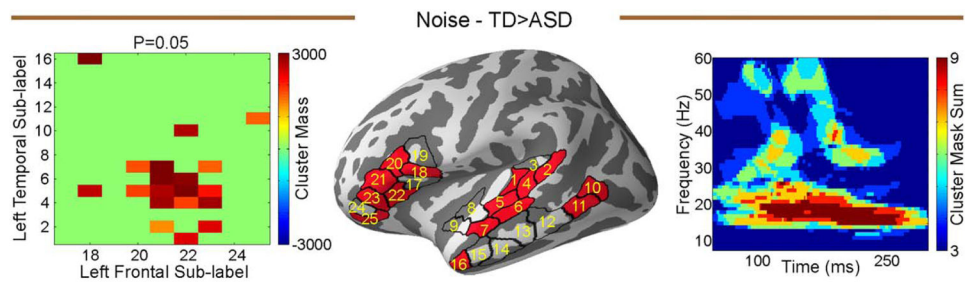


Figure 4.

Group comparison of normalized coherence (deviant normalized by standard) during the noise condition, between TD and ASD. Left panel is the matrix of sub-label pairs that reached significance, the middle panel shows those labels on the cortex, and the right panel is the time frequency map of the sum of the cluster masks between the significant sub-labels from left panel.

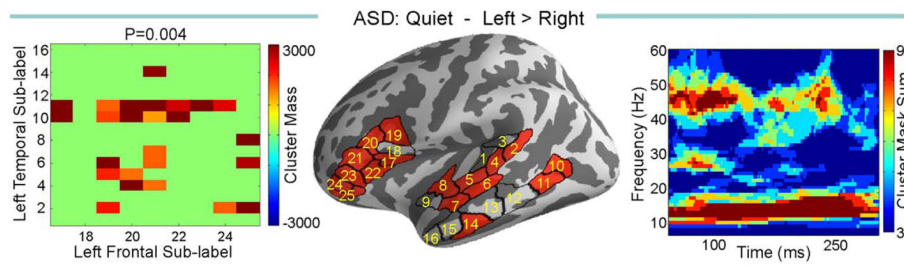


Figure 5.

Comparison of left versus right normalized coherences within ASD group in the quiet. Left panel is the matrix of sub-label pairs that reached significance, the middle panel shows those labels on the cortex, and the right panel is the time frequency map of the sum of the cluster masks between the significant sub-labels from left panel.

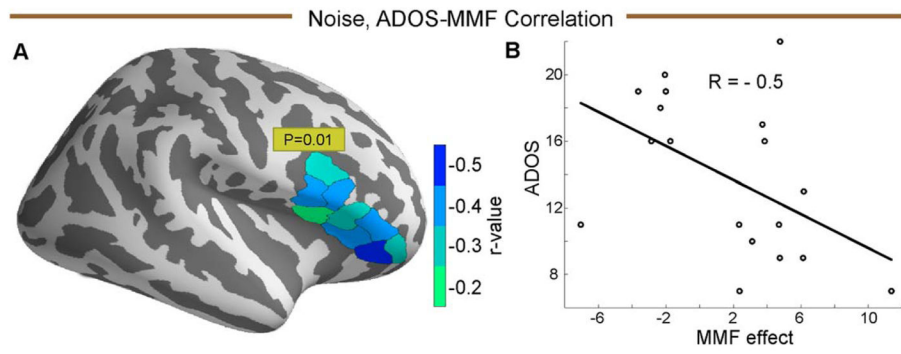


Figure 6.

(A) The sub-labels in rIFG sub-labels, that correlated with the total ADOS score, in the noise condition, color coded by the sub-label correlation value (r). (B) ADOS-MMF correlation plot for the sub-label with minimum negative correlation value.

Table 1

Behavioral Scores and Demographic Information for TDs and ASDs

	Age	Verbal IQ	Non-verbal IQ	ADOS
	Mean ± SD	Mean ± SD	Mean ± SD	Mean ± SD
TD (n = 17)	12 ± 3	115 ± 14	112 ± 17	1.7 ± 1.8
ASD (n = 19)	13 ± 2	110 ± 25	100 ± 17	13.7 ± 4.7
P-value (TD vs. ASD)	n.s	n.s	0.04	6e-11

n.s stands for non-significant.

Author Manuscript

Author Manuscript

Author Manuscript

Author Manuscript